

# Segmented Soft Pneumatic Bending Actuator with Artificial Neural Network for Parameter Prediction

Mark Joseph B. Enojas and Manuel C. Ramos Jr.

**Abstract**—Most of the models of soft robotic gloves can do flexion and extension. However, there are other hand rehabilitation exercises such as tendon glide which requires variations of finger pose. It cannot be done with just a single motion of flexion or extension. Individual joint control is needed in order to achieve the normal-to-maximum range of motion when doing the hand exercises. In this paper, a design of a segmented soft pneumatic bending actuator (sPBA) with individual joint control using PID with Artificial Neural Network (ANN) for parameter prediction is presented. Each joint has its individual inlets and has pneumatic chambers that bends when supplied with air. A pneumatic control setup is developed to control the three finger joints; the Metacarpophalangeal (MCP), Proximal Interphalangeal (PIP), and the Distal Interphalangeal (DIP). Varying the air pressure supplied to the joints achieves different bending positions of the finger. An experimental setup was developed in order to characterize and gather data that is used to develop ANN for predicting the bending angle-to-pressure parameter. A total of 2197 images are captured from the different combinations of pressure which are equivalent to different bending angles. A simple PID control was used to achieve the desired bending. The setup has a mean-square-error (MSE) of 1.85007 at validation with overall R of 0.9994 and a maximum error of 5.4 kPa pressure in joint 1 at low pressure. This setup will be useful to develop a soft robotic rehabilitation glove.

**Index Terms**—Artificial neural network, soft pneumatic bending actuator, hand rehabilitation, hyper redundant actuator, soft robotic glove.

## I. INTRODUCTION

The vast development of soft robotic structures and systems contributes to innovations for biomedical applications. The growing demand of physical and occupational therapists gives the scientists and engineers the ideas of developing soft robotics for hand rehabilitation. Rehabilitation is trying the least invasive option that has shown to be just as effective for their condition [1]. However, most rehabilitative hand exercises, such as tendon gliding and nerve flossing, require different positions of the fingers.

In order to achieve such positions, individual control and segmentation for each joint is required [2]–[6]. Rehabilitation gloves are significant in both cases of active and passive hand exercises [7]. Several soft pneumatic actuators exist in

different designs and structures[8]–[10]. Most of these models primarily perform flexion and extension from a single source of pneumatic pressure for a single actuator network design resulting in limited finger exercises.

It is difficult to model soft actuators mathematically because of its high nonlinear characteristics. This enables the application of ANN for predicting parameters of the sPBA[11], [12]. In this paper, a segmented sPBA is developed which is able to perform different finger rehabilitation exercises. Varying the combinations of air supply pressure to each of the actuator joints enables it to perform different finger flexion and extension exercises. An ANN is set up in order to translate the bending angle-to-pressure parameters for the sPBA to achieve its desired planar pose.

The succeeding sections discuss the following: Section II discusses the design of segmented actuators with separate inlets for each joint, the experimental setup, the process of extracting coordinates and bending angle of each of the joints of the actuator, and the ANN setup for estimating pressure for the desired actuator positions, and Section III discusses the experimental results and the performance of the ANN setup.

## II. METHODOLOGY

### A. sPBA Design and Finite Element Method (FEM) Simulation

It is necessary to do simulation to achieve the best actuator response in designing sPBA. A FEM software is used to simulate the response of the actuator in ideal parameters. The following parameters are used based on characteristics of the silicone Elastosil M4601: the density of 1130 kg/m<sup>2</sup>, the Yeoh coefficient of  $C_{10}=0.11$  and  $C_{20}=0.02$ , and a gravity of 9.81 m/s<sup>2</sup>. Each joint is composed of 3 pneumatic networks which will bend when inflated with compressed air. The symmetric structure is designed to ideally avoid elongation and twisting of the actuator as in [4]. The inflated chambers allow the side walls of the sPBA to create a bending mechanism. See Figure 1 for the FEM model of the actuator.

The links in between the MCP, PIP, and DIP joints are segmented so that it may resemble the human finger. This is beneficial in coupling the sPBA to the fingers of the user. The link lengths and the node assignments are based on the geometric mesh developed upon simulation. There are 6 working nodes and links in the designed sPBA.

There are three air inlets that run in the base of the sPBA for the air distribution across the joints. A combination of different air pressure supplies is applied in each joint in step increments of 10 kPa. A kinematic equation will be used to compute the bending angle using the node coordinates.

Manuscript received April 15, 2021; revised December 21, 2021. This work is funded through the program of Engineering Research and Development for Technology by the Department of Science and Technology-Science Education Institute of the Philippine Government.

The authors are with the Robotics and Automation Laboratory of the Electrical and Electronics Engineering Institute of the University of the Philippines Diliman, Quezon City, Philippines (e-mail: mark.joseph.enojas@eee.upd.edu.ph, manuel@eee.upd.edu.ph).

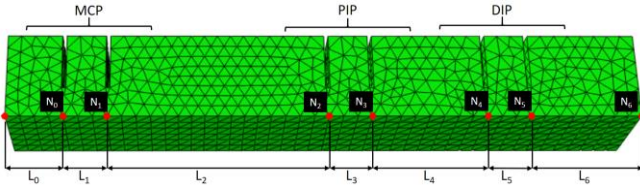


Fig. 1. Segmented sPBA mesh with assigned nodes and links for the MCP, PIP, and DIP joints.

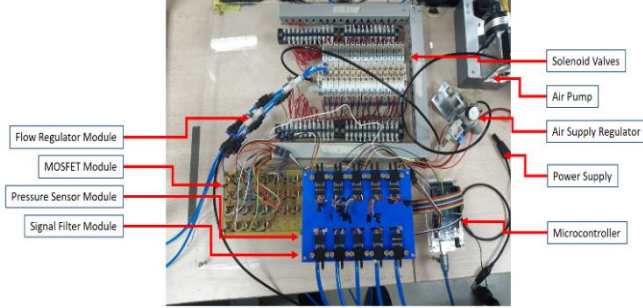


Fig. 2. Control board.

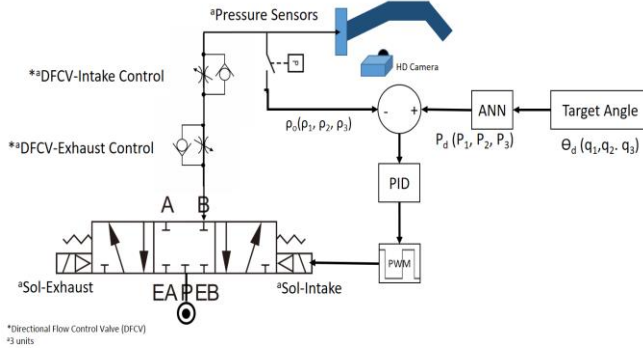


Fig. 3. Control system diagram.

### B. Experimental Setup

Fig. 2 shows the control system which is composed of a control board and the evaluation platform. The control board is made up of the following: 1) solenoid valves, 2) pneumatic sensor module, 3) air pump and air regulator, 4) MOSFET module, 5) signal filter module, 6) microcontrollers, and 7) power supply modules. The solenoid valves are controlled through pulse width modulation (PWM) to regulate the pressure. A simple proportional, integral, and derivative (PID) control setup was established to control pressure. See Figure 3 for the control system diagram.

Two microcontrollers were used; Arduino ATMEGA 2560 for pressure control, and Raspberry Pi 3 for capturing and processing of images. A high definition camera is used to capture the image programmed in OpenCV. This camera is calibrated before it is used in the setup in order to eliminate distortion. When the pressure combination is achieved, a photo will be captured and stored in a folder. These images will be processed for the extraction of the coordinates and for the computation of the bending angle using the kinematic equation.

### C. Kinematics of Hyper Redundant Structure

The kinematic equation for the actuator is derived using the assumption of a hyper redundant structure. This can simply be understood by creating small rigid and straight structures out of a curvature. The more nodes that are assigned, the more accurate the measurement. Applying this to a nonlinear

structure sPBA, the estimation of the bending angle is possible. Table I presents the parameters needed for developing the kinematic equation. The link lengths are assumed to be ideally unchanging, where there is no extension or compression.

TABLE I: STRUCTURAL KINEMATICS AND MASS PARAMETERS

$i$	$a_i$ (mm) <sup>a</sup>	$m_i$ (gm)	$d_i$ (mm)	$\alpha_i$ (deg)	$\Theta_i$ (deg)
1	$a_1$	3.5	0	0	$\Theta_1$
2	$a_2$	21.1	0	0	$\Theta_2$
3	$a_3$	3.5	0	0	$\Theta_3$
4	$a_4$	10.2	0	0	$\Theta_4$
5	$a_5$	3.5	0	0	$\Theta_5$
6	$a_6$	10.5	0	0	$\Theta_6$

<sup>a</sup> Assumed unchanging:  $a = [10.8, 49.2, 10.8, 25.2, 10.8, 24.6]$

Equation (1) is the transformation matrix for a revolute joint. This is used to derive the kinematic equation (2). The actuator has a 2D planar movement where the z-coordinate component is ideally zero. Equation (3) is used to estimate the coordinates of the assigned nodes, noting that  $i = 1, 2, 3, \dots, n - 1$  and considering the origin is at (0,0) as node 1. To determine the coordinates of the tip of the actuator,  $p_x, p_y, p_z$ , (4) is used.

$$A_{i-1}^i = \begin{bmatrix} \cos \theta_i & -\cos \alpha_i \sin \theta_i & \sin \alpha_i \sin \theta_i & a_i \cos \theta_i \\ \sin \theta_i & \cos \alpha_i \cos \theta_i & -\sin \alpha_i \cos \theta_i & a_i \sin \theta_i \\ 0 & \sin \theta_i & \cos \alpha_i & d_i \\ 0 & 0 & 0 & 1 \end{bmatrix} \quad (1)$$

$$P = A_0^1 A_1^2 \dots A_{n-1}^n \begin{bmatrix} 0 \\ 0 \\ 0 \\ 1 \end{bmatrix} \quad (2)$$

$$P_i = \begin{bmatrix} p_{x_i} \\ p_{y_i} \\ p_{z_i} \end{bmatrix} \quad (3)$$

$$= \begin{bmatrix} x_{i+1} - L_i \cos(\theta_1 + \theta_2 + \dots + \theta_i), i = 2, 3, \dots, n - 1 \\ y_{i+1} - L_i \sin(\theta_1 + \theta_2 + \dots + \theta_i), i = 2, 3, \dots, n - 1 \\ 0 \end{bmatrix}$$

$$\begin{bmatrix} p_x \\ p_y \\ p_z \end{bmatrix} = \begin{bmatrix} \sum_{i=1}^n L_i \cos \sum_{j=1}^i \theta_j \\ \sum_{i=1}^n L_i \sin \sum_{j=1}^i \theta_j \\ 0 \end{bmatrix} \quad (4)$$

### D. ANN Setup

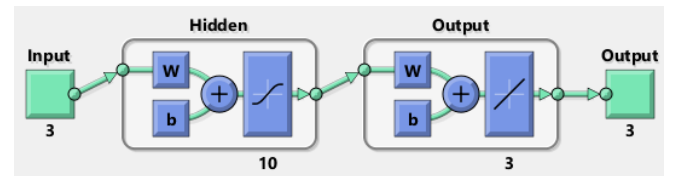


Fig. 4. Artificial neural network setup.

An ANN is set up to act as the inverse kinematic solution to bending angle-to-pressure prediction of the sPBA behavior. The combination of the three bending angles desired for each joint are the inputs, and its equivalent pressures are the outputs. A hidden layer with 10 neurons and a hyperbolic tangent sigmoid symmetric transfer function (5) was set up in

a feedforward back propagation network type. See Fig. 4 for the ANN setup.

$$a = \frac{2}{(1 + e^{-2n})} - 1 \quad (5)$$

### III. RESULTS AND DISCUSSION

#### A. FEM Simulation

There were six links assigned in the designed sPBA. The nodes are assigned based on the mesh generated in the FEM simulation. A pressure approximately 170 kPa is able to achieve nearly 90° bending. The bending structure is illustrated in Fig. 5. The MCP, PIP, and DIP joints are labeled as J1, J2, and J3 respectively. The results show the achieved bending for a full fist tendon glide exercise. The equivalent bending angle for each joint is the combination of  $\Theta_1$  and  $\Theta_2$ ,  $\Theta_3$  and  $\Theta_4$ ,  $\Theta_5$  and  $\Theta_6$ , for J1, J2, and J3 respectively. See Fig. 5b for the joint configuration.

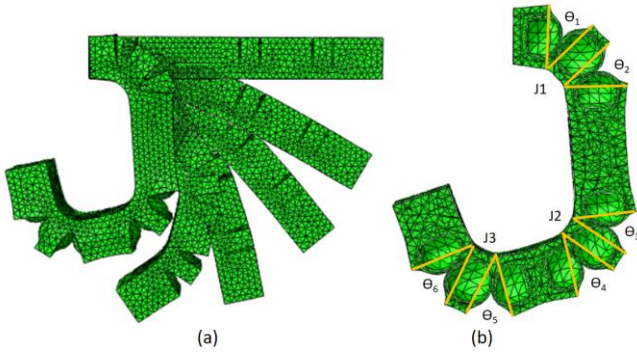


Fig. 5. (a) FEM simulation with pressure of 170 kPa for each joint, (b) joint bending angle configuration.

#### B. Experimental Results

A total of 2197 images were extracted in unique combinations of pressure supplied in each joint in a 10 kPa increment. Markers were installed in the sPBA to locate the nodes assigned for each joint similar to the nodes assigned in the FEM setup. Compared to the FEM simulation, the sPBA approximately achieves a bending angle of 90o at 120 kPa. Fig. 6 shows the captured images supplying each joint with uniform pressures to all the joints: 20, 40, 60, 80, 100, 120 kPa.

The developed actuator is embedded in a neoprene glove. This is done by putting Velcro fastening tape along the link attachments. See Fig. 7 for the sPBA attachment to the glove. In this experiment, two sPBA actuators are installed in the index finger and middle finger.

#### C. ANN Training and Validation

An error of 5.4 kPa in joint 1 is the maximum error attained in the ANN setup. The data set distribution is 60%, 20%, 20%, for training, validation, and test set respectively, which are based on the cross validation partition with Levenberg Marquardt training algorithm. Fig. 8 shows the error histogram with the distribution of instances of the partitioned data set for training, validation, and test data. The higher deviation positive and negative values exist in the low pressure combinations. These are the pressure supplies from 20 kPa and below. This phenomenon is due to the pre-bending of the actuator due to the influence of gravity. Six

validation checks were incurred upon training of the ANN as illustrated in Fig. 9.

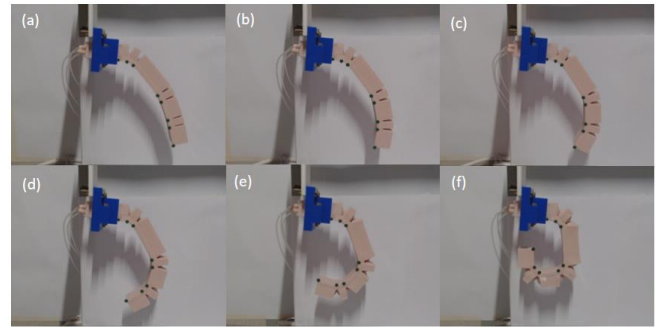


Fig. 6. Actuator bending in different air pressures [20:40:60: 80:100:120].

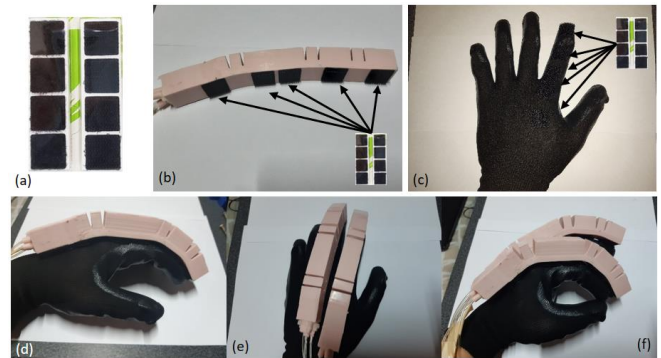
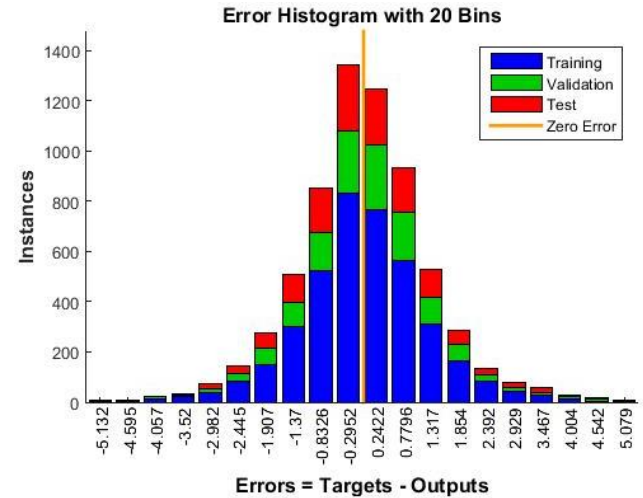


Fig. 7. sPBA attachment to the glove. (a) Velcro fastening tape by Polar Bear, (b) Velcro attachment to the sPBA, (c) Velcro attachment to the glove, (d) adjoining the sPBA and the glove, (e-f) sPBA for index and middle finger.



Errors = Targets - Outputs

Fig. 8. Error histogram.

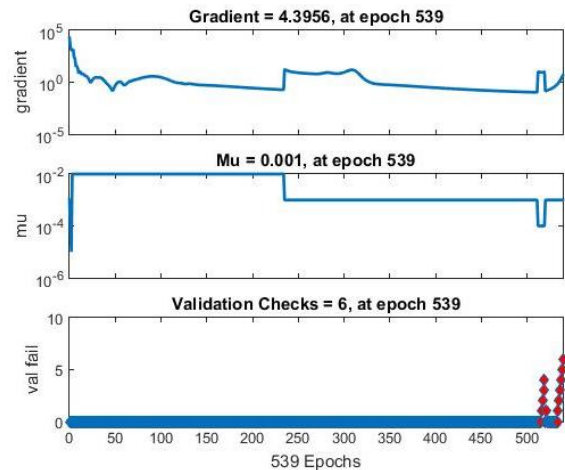


Fig. 9. ANN training.

The three pressure parameters for each joint attained the best validation performance of MSE at 1.8506 which shows that the model complexity runs well as shown in Fig. 10. Both the training and validation errors rest low to keep good prediction performance. The ANN setup has low variance and low bias which makes it a good model.

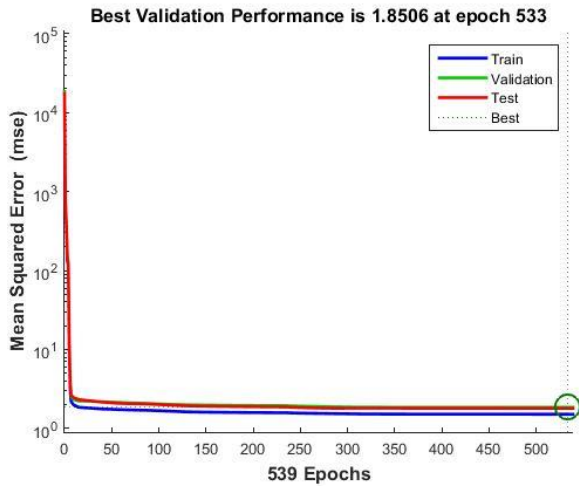


Fig. 10. ANN performance.

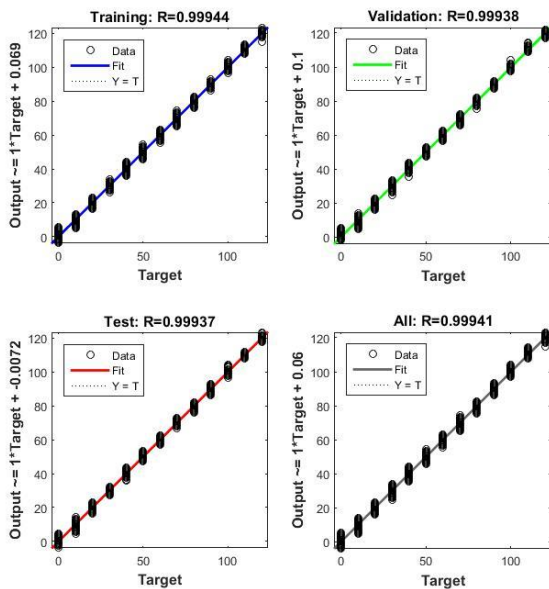


Fig. 11. Regression plot.

TABLE II: ANN TRAINING RESULTS

Set	Samples	MSE	R
Training	1319	1.51397e <sup>0</sup>	0.999443
Validation	439	1.85062e <sup>0</sup>	0.999378
Testing	439	1.80119e <sup>0</sup>	0.999370

The regression plot shown in Fig. 11 shows that there are no outliers, rather the error is small enough and acceptable that the ANN is able to generalize. The ANN training result can be summarized by the MSE and regression R values in Table II. Several trials have been conducted to cross validate the ANN. With 2197 samples, the MSE is at 1.85 for the validation set. An MSE below 2 is of good performance.

The maximum pressure errors in the positive and negative regions are 5.3447 kPa in joint 1 and -5.402 kPa in joint 3 respectively. Fig. 12 presents the error plot of the three joints. The maximum percent error is at joint 1 at 53.47%. See Fig. 13 for the percent error plot. This spike in error is due to the

pre-bending of the sPBA at low air pressure supply due to the gravity. This error is negligible when the application is for higher pressure operations of bending the sPBA.

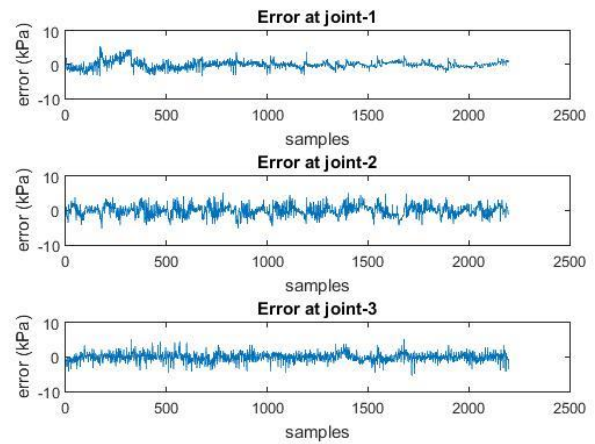


Fig. 12. Error plot for the three joints.

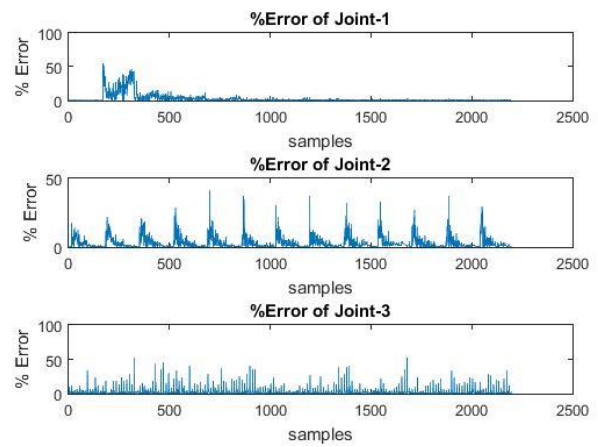


Fig. 13. Percent error plot for the three joints.

#### IV. CONCLUSION AND FUTURE WORK

Different finger exercises can now be achieved through the developed segmented sPBA by varying the individual pressure supply in each of the joints. The ANN setup used in this study was able to predict the equivalent air pressure of the desired actuator bending angle pose. The 2197 samples collected are enough to train the ANN. It has an acceptable maximum error of 5.4 kPa at joint 1 with an overall R=0.99944. At low pressure, the maximum percent error is 53% which is caused by the pre-bending of the actuator due to gravity. This setup can be useful for the development of a soft robotic glove for rehabilitation that is able to perform different finger and hand exercises.

In the future, the sPBA design and setup will be used to develop a soft robotic glove that can be used for hand rehabilitation, able to do different functional exercises for the ADL. The gripping force will be analyzed to study the effect on the patient's development based on different hand motor assessment scales.

#### CONFLICT OF INTEREST

The authors declare no conflict of interest.

#### AUTHOR CONTRIBUTIONS

M. J. B. Enojas conducted the study and experiments. He

also wrote this manuscript. M. C. Ramos is the adviser in conducting this study. All the authors have approved the final revision of this paper.

#### REFERENCES

- [1] T. Goggins, "Rehabilitation of the hand," *Orthop. Trauma*, vol. 33, no. 1, pp. 62–65, 2018.
- [2] J. Wang, Y. Fei, and W. Pang, "Design, modeling, and testing of a soft pneumatic glove with segmented pneunets bending actuators," *IEEE/ASME Trans. Mechatronics*, vol. 24, no. 3, pp. 990–1001, 2019.
- [3] P. Polygerinos *et al.*, "Towards a soft pneumatic glove for hand rehabilitation," *IEEE Int. Conf. Intell. Robot. Syst.*, pp. 1512–1517, 2013.
- [4] M. J. B. Enojas and M. C. Ramos, "Development of a finger soft pneumatic bending actuator," in *Proc. 2019 4th Asia-Pacific Conference on Intelligent Robot Systems*, 2019, pp. 1–5.
- [5] H. L. Heung, Z. Q. Tang, X. Q. Shi, K. Y. Tong, and Z. Li, "Soft rehabilitation actuator with integrated post-stroke finger spasticity evaluation," *Front. Bioeng. Biotechnol.*, vol. 8, pp. 1–10, 2020.
- [6] P. Polygerinos, K. C. Galloway, E. Savage, M. Herman, K. O'Donnell, and C. J. Walsh, "Soft robotic glove for hand rehabilitation and task specific training," in *Proc. IEEE Int. Conf. Robot. Autom.*, pp. 2913–2919, 2015.
- [7] A. Rashid and O. Hasan, "Wearable technologies for hand joints monitoring for rehabilitation: A survey," *Microelectronics J.*, vol. 88, pp. 173–183, 2019.
- [8] H. Wang, M. Totaro, and L. Beccai, "Toward perceptive soft robots: progress and challenges," *Adv. Sci.*, vol. 5, no. 9, 2018.
- [9] Y. Hao *et al.*, "Modeling and experiments of a soft robotic gripper in amphibious environments," *Int. J. Adv. Robot. Syst.*, vol. 14, no. 3, pp. 1–12, 2017.
- [10] P. Polygerinos *et al.*, "Modeling of soft fiber-reinforced bending actuators," *IEEE Trans. Robot.*, vol. 31, no. 3, pp. 778–789, 2015.
- [11] K. Elgeneidy *et al.*, "Sciedirect data-driven bending angle prediction of soft pneumatic actuators with embedded soft bending

- angle actuators with with embedded flex sensors," *IFAC-PapersOnLine*, vol. 49, no. 21, pp. 513–520, 2016.
- [12] N. Lohse, K. Elgeneidy, N. Lohse, and M. Jackson, "Bending angle prediction and control of soft pneumatic actuators with embedded flex sensors - A data-driven approach," *Mechatronics*, p. 1, 2017.

Copyright © 2022 by the authors. This is an open access article distributed under the Creative Commons Attribution License which permits unrestricted use, distribution, and reproduction in any medium, provided the original work is properly cited ([CC BY 4.0](https://creativecommons.org/licenses/by/4.0/)).



**Mark Joseph B. Enojas** received a degree in B.S. electronics and communications engineering from the Technological University of the Philippines Taguig in 2009 and master of information technology from the University of the Philippines Los Baños in 2013. He is currently pursuing his Ph.D. degree in electrical and electronics engineering in the University of the Philippines Diliman. His research interests are on soft robotics for biomedical applications. It includes the application of control systems and various methods and solutions in analyzing nonlinear behavior of soft actuators.



**Manuel C. Ramos Jr.** received his Ph.D. degree in electrical engineering from Purdue University in 1998. He is a professor in the Electrical and Electronics Engineering Institute of the University of the Philippines Diliman. He is currently the director at the University Computer Center of the said university. His research interests are on control systems, nonlinear control, robotics, and fuzzy systems. His recent publications are on controller architectures of autonomous vehicles.